Finite element analysis of over-height vehicle collisions on prestressed girder bridges

A. Samadzad, S. Cathey, M. Whelan, N. Braxtan, & S. Chen
University of North Carolina at Charlotte, Charlotte, N.C., U.S.A.

ABSTRACT: The accidental collision of over-height vehicles, especially construction equipment hauled on trailers and dump trucks with unintentionally raised beds, with bridge girders is an event that often occurs multiple times a year in many states within the U.S. The evaluation of bridges subjected to over-height impacts is typically informed by visual inspection, however some damage mechanisms having significant effects on the strength and durability of prestressed concrete girders may not be visually apparent and therefore can be difficult to assess. Furthermore, the damages resulting from an over-height vehicle collision, and subsequent repair and replacement implications, are dependent on the nature and speed of the offending vehicle and the characteristics of the bridge subjected to the impact force. In this paper, a framework for high fidelity finite element analysis of over-height vehicle collisions with prestressed concrete girder bridges is developed to provide a physics-based approach for predicting the damages from over-height vehicle impacts and the influence of the damage on the residual capacity. When coupled with field observations, high fidelity finite element analysis can provide a means for improving post-impact damage assessments and avoiding unnecessary repair and replacement actions while mitigating potential safety risks. The paper details the modeling strategies and constitutive models adopted to create finite element models of conventional prestressed concrete girder bridges, demonstrates the automatic generation of finite element models from key parameters of bridge plans, and presents simulation results for a representative bridge to examine the influence of over-height vehicle characteristics and speed on the predicted extent of damage.

1 INTRODUCTION

According to a recent analysis of a regional database of bridge failures in the United States, collisions are the second most common cause of bridge failures, with the failure typically occurring as a partial collapse (Cook et al. 2015). However, the majority of collisions of over-height vehicles and carried freight with bridges result in minor or moderate damage that can be repaired (Feldman et al. 1996), although often at significant cost and with potentially lengthy disruption to service. In 2020 alone, 14,630 vehicle collisions with bridges were reported throughout the United States (National Center for Statistics and Analysis 2022). Statistical analysis of a large database of bridge collision incidents in New York State indicated that over-height vehicle collisions are significantly more prevalent than vehicle collisions with abutments or piers. Furthermore, the majority of over-height collisions were attributed to trucks and trailers carrying construction equipment, materials, and other objects (Agrawal et al. 2011).

Experimental insight on the behavior of prestressed concrete girder bridges under lateral impacts has been extremely limited. The few exceptions include laboratory testing of model-scale partial width bridge spans to investigate the effect of intermediate diaphragm type and location (Abendroth et al. 1995) and a single experimental test of a full-scale girder subjected to lateral impact from a large concrete mass carried by a cart (Jing et al. 2016). The latter experiment was conducted with an independent girder and therefore does not reflect the contributions that end diaphragms, intermediate diaphragms, additional girders, and a complete deck would provide in an actual bridge, while the former experiment relied on quasistatic loading as a substitute to impact loading. Due to technical and logistical challenges, risks, and significant costs associated with impact testing of full-scale bridge girders, finite element (FE) analysis has been the predominant tool for investigating the behavior of bridges under impact loads and understanding the effect of design features and impactor characteristics on the resulting severity of damage.

A significant portion of earlier research on the response of prestressed concrete girder bridges to over-height collisions centered on the role of intermediate diaphragms and effect of the diaphragm design on the lateral resistance of the bridge (Abendroth et al. 1995, Qiao et al. 2008). However, FE analysis that served as the basis for this early research was hindered by the technological capabilities of the time as reflected by coarse meshes, simplified constitutive models, idealized boundary conditions, absence of strain-rate effects, neglect of bent diaphragms and other bridge components that may contribute to the girder resistance, and simplified modeling of the impact through prescribed force time histories rather than explicitly modeling the impacting object with a contact model. A critical review prepared subsequent to much of this early research classified the effect of diaphragms during lateral impacts as “not fully addressed” and recommended that high-fidelity modeling be pursued to overcome the limitations of imposed by the computational simplifications (Cai et al. 2007).

Recently, the investigation of over-height vehicle impacts to bridge girders has experienced renewed interest with the support of high-fidelity FE analysis with advanced constitutive models. Xu et al. (2013) developed FE models for container, tipper, and tank trucks and simulated the collision of these vehicles with a prestressed concrete girder bridge model to investigate damage mechanisms and impact force characteristics as well as to develop a simplified model to predict the collision force time history. Oppong et al. (2021a) conducted parametric analysis of the collision of several construction objects as well as a tractor-semitrailer with reinforced concrete bridge girders to investigate variations in impact forces and girder damage. Simplified equations were developed to predict the impact force characteristics for concrete pipe and steel tank collisions. This work was extended to reinforced concrete bridge girders constructed with high-strength concrete and ultrahigh-performance concrete (Oppong et al. 2021b). The numerical simulations suggest that the mean impact force is greater for collisions with ultrahigh-performance concrete girders, but the lateral displacement and resulting damage is reduced.

2 AUTOMATED MODEL GENERATION AND MODELING APPROACH

This paper discusses the development of high-fidelity FE models of complete bridge superstructures to investigate the influence of bridge and impacting object characteristics on the severity of damage to prestressed concrete girders. LS-DYNA was selected by the authors as the FE analysis software package for the research and all simulations disclosed in this paper are conducted using the explicit time integration scheme.

2.1 *Automated model generation*

The construction of large, detailed FE models can be a time-consuming exercise and ensuring consistency in the modeling technique and assignment of model parameters is extremely challenging when a set of FE models are created manually. To address this challenge and to facilitate rapid development of parametric models, the authors have written an extensive library of MATLAB scripts to automatically prepare LS-DYNA keyword files using a defined structure of geometric and material properties that can be extracted from bridge plans. The library is capable of automatically generating keyword files for highly detailed FE models of prestressed concrete girder bridges, implementing the modeling approach and staged analysis sequence described in the subsequent sections, with no manual intervention or manipulation of the keyword files prior to the analysis.

2.2 *Description of finite element modeling approach*

The concrete in the girders is modeled using constant stress hexahedral solid elements with the Continuous Surface Cap Model (CSCM) used for constitutive modeling of the nonlinear, inelastic, and strain-rate dependent behavior of the concrete. CSCM has been found to provide realistic predictions for the behavior of reinforced concrete members subjected to impact loading (Adhikary et al. 2005, Saini and Shafei, 2019). Automatic parameter generation for this constitutive model is available in LS-DYNA requiring only the mass density, maximum aggregate size, and unconfined compressive strength of the concrete. A database of 2D meshes for standard girder cross sections has been developed by the authors using HyperMesh to ensure high element quality while constraining the minimum edge size to prevent a small number of elements from establishing an unnecessarily small time step. These 2D meshes are then used to create the 3D meshes for the girders by replicating the node set and connectivity at uniform increments along the length of each girder. Prestressing strands are modeled using truss elements with a plastic kinematic material model implemented with yielding and isotropic hardening. Mild reinforcement is similarly modeled as a plastic kinematic material, although Hughes-Liu beam elements are used to ensure stability of shear reinforcement that is not fully embedded in concrete prior to the introduction of the deck. Both the prestressing strand and the mild reinforcement include strain-rate effects using the Cowper and Symonds model. The constrained beam in solid constraint is used to couple the strands and reinforcement to the concrete in the model. Sole plates at the bearing surfaces are modeled with shell elements assigned to shared nodes with the concrete elements in the girder. This effectively permits the ability to prescribe both translational and rotational boundary conditions using a single node at the bearing location.

The reinforced concrete deck is modeled with constant stress hexahedral solid elements. Shared nodes are used to couple the girders to the deck. End and continuous bent diaphragms are also modeled with constant stress hexahedral solid elements. Given the difficulty in generating a mesh for the bent diaphragms that would share nodes with the girder elements without introducing small or highly distorted elements, tied nodes to surface contact was used to couple the bent diaphragms to the girders. A similar approach is used to model cast-in-place reinforced concrete diaphragms. For simplicity, the authors adopt an elastic material model for the deck and bent diaphragms under an assumption that the bridge deck and bent diaphragms will experience little to no damage from lateral impact to the girder. For bridges with steel intermediate diaphragms, the channel member and connecting plates are modeled with shell elements. For bridges with X-brace with strut intermediate diaphragms, Hughes-Liu beam elements are used to model the individual members of each diaphragm. Steel intermediate diaphragms are modeled with the plastic kinematic material model and include yielding, isotropic hardening, and strain-rate dependency.

2.3 *Description of analysis sequence*

To accurately initialize the internal state of stress and initial camber in the complete bridge model, a staged development of the FE models that replicates aspects of the construction sequence is required. Specifically, prestressed concrete girder bridges are constructed of girders that are prestressed prior to placement at the site and then the diaphragms, deck, and remaining bridge components are placed or cast. Consequently, it is necessary to introduce the effects of prestressing in a model that initially consists of just the girders so that the bridge deck does not act compositely with the girders during the introduction of prestressing, as the contribution of the deck would significantly affect the stress, neutral axis location, and camber in the model. A schematic representation of the staged development of the FE model is presented in Figure 1. The staged initialization of the full bridge model is accomplished by using the full restart capability of LS-DYNA. Advantageously, the full restart feature only requires initialization of the bridge model once. Multiple impact analyses can be performed on the initialized model by consistently restarting from the d3dump file created at the conclusion of Step 2.

The introduction of prestressing force in this study was based on applying an equivalent temperature-induced shrinkage in the elements representing the prestressing strands. This general approach was detailed in Jiang and Chorzepa (2015), however the equation provided for the temperature change in this source does not account for elastic shortening. When elastic shortening is included in the strain compatibility, the temperature change, ΔT, associated with a desired prestressing force, f, in the model is:

$$\Delta T = \frac{f}{\alpha}\left(\frac{1}{E_s A_s} + \frac{1}{E_c A_c} + \frac{e^2}{E_c I_c}\right) \tag{1}$$

where α is the temperature coefficient, E_s is the modulus of elasticity for the strands, E_c is the modulus of elasticity for the concrete, A_s is the cross sectional area of the strands, A_c is the cross sectional area of the concrete, I_c is the moment of inertia of the concrete, and e is the eccentricity of the strands. The desired prestressing force introduced into the model can account for typical prestress losses, which can be estimated specifically for the age of the structure at the time of the simulated impact. The application of the prestress in the model is applied simultaneously with the introduction of body forces due to gravitational acceleration during a transient analysis with explicit time integration. This analysis extends over a multiple of the natural period of the girder associated with the fundamental mode for major axis flexure. Mass proportional damping is applied at this stage to suppress resonance of the vibrational modes during the application of the static loads. During the introduction of the prestress force, idealized boundary conditions are assigned at the bearing locations.

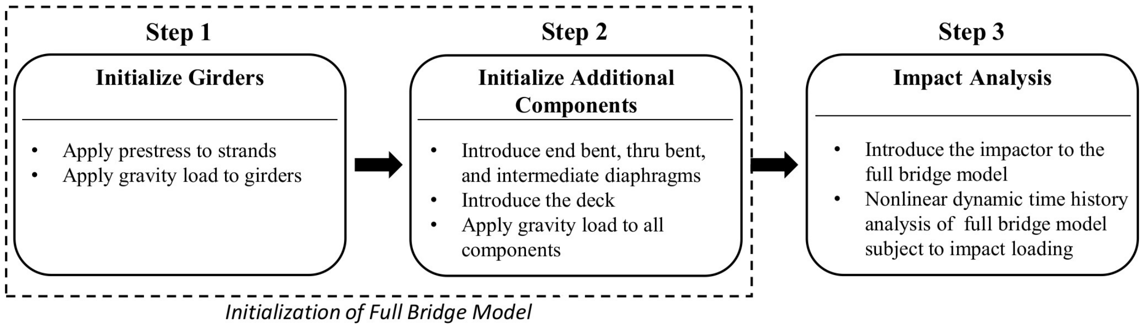

Figure 1. Staged development and analysis of prestressed concrete girder bridge models.

Following the initialization of the individual girders, the remaining bridge components are introduced to the model. During this second step of the initialization of the bridge model, the idealized boundary conditions are replaced with linear elastic translational and rotational springs to approximate the behavior of the elastomeric bearings. The springs are introduced in LS-DYNA using the linear elastic discrete beam material model and the spring stiffnesses are calculated for compressive, shear, flexural, and torsional behavior of the steel-reinforced elastomeric bearings using AASHTO-based guidance outlined in Whelan & Janoyan (2011). The second step of the model initialization introduces the body forces in the added components due to gravitation acceleration as well as establishes equilibrium of the model with the elastic boundary conditions. At the conclusion of this step, mass proportional damping is removed from the model, the impacting object and associated contact model are introduced, and transient analysis is conducted to simulate the damage to the bridge resulting from the collision.

2.4 *Details of bridge span used as a case study*

As detailed above, the developed library of scripts automates the development of high-fidelity models of prestressed concrete bridges, which will ultimately facilitate parametric analysis of the effect of bridge and impacting object characteristics on the severity of damage to prestressed concrete girder bridges. In this paper, a case study of a FE of a single bridge span created by the developed library of scripts is presented and preliminary results from impact simulations are discussed. The bridge span modeled in this paper is a representation of an actual design from the bridge inventory of the State of North Carolina with all geometric and material properties sourced from bridge plans.

The bridge span consists of six AASHTO Type IV girders spaced 2.46 m on-center and spanning 23.72 m. The span has a 10° skew, a crown point at the center of the cross section with symmetric 2% slope on each side of the crown point, and an out-to-out width of 14.5 m. The reinforced concrete deck is 210 mm thick. Each girder is prestressed with a total of 26 low relaxation grade 1860 (270) strands of 15.24 mm diameter. All strands in the girders are straight and bonded over the full length of the span. The compressive strength of the concrete in the girders is 41.4 MPa and the maximum aggregate size is 8 mm. The girders include additional longitudinal reinforcing steel at the ends and near the connection to intermediate diaphragms as well as shear reinforcement along the span. The girders are supported by rectangular steel reinforced elastomeric bearings with one bearing being designed as an expansion bearing to accommodate thermal expansion. Intermediate diaphragms comprised of steel channels bolted to angle connector plates are present at the midspan of the girders. The span includes reinforced concrete partial depth end bent diaphragms and full depth continuous bent diaphragms. The mass density of all concrete materials in the model was taken as 2,400 kg/m^3, while the mass density of all steel materials in the model was taken as 8,000 kg/m^3. An edge size of 50 mm was used to develop the mesh for the FE model of this bridge span.

Figure 2 presents the bridge model as well as the vertical displacement in the model after the staged initialization. The positive displacement at the midspan of the girder predicted by the FE analysis was verified through comparison with the calculated camber as well as estimates provided on the bridge plans. It is noted that the negative displacements throughout the bridge deck are generated due to the introduction of the deck to the model after the introduction of prestressing to the girders, consistent with the construction sequence. The downward displacement reflects the deflection resulting from the self-weight of the deck and intermediate diaphragms.

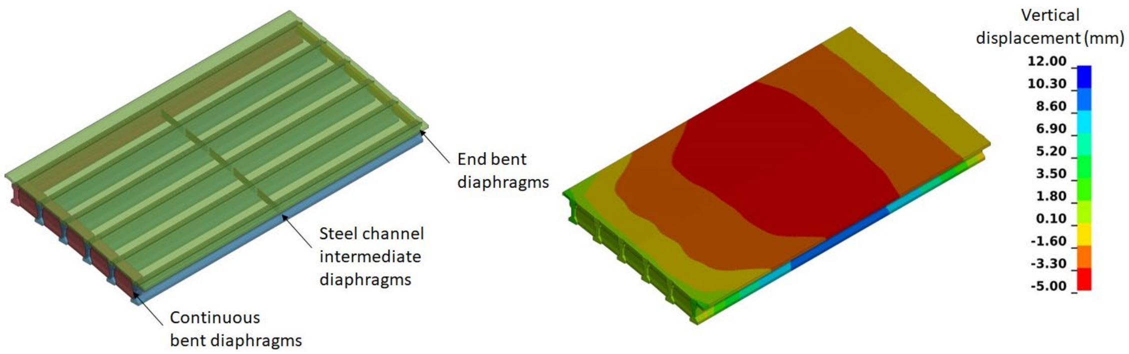

Figure 2. FE model of prestressed concrete bridge: a) rendering of components in model; b) vertical displacement after staged initialization of the model.

3 IMPACT SIMULATIONS

A recently published study utilized high-fidelity FE analysis to examine the variation in impact forces and develop simplified equations to predict the peak and mean force of the impactor (Oppong et al. 2021a). In the authors' opinion, this study established a benchmark for high fidelity modeling of overheight collisions to bridge girders. However, the study was limited to reinforced concrete girders and, furthermore, the database of simulations used to develop the simplified equations was based on a single span length. Prior to conducting the current study, the authors replicated the results in the referenced paper to ensure that the modeling approach, assumptions, and parameters used were consistent with those used by the other authors. In the current study, the authors adopt the geometry and modeling strategies for the steel tank and concrete pipe impacting objects detailed in this referenced publication. The steel tank model is a closed ended hollow cylinder with an outer diameter of 2.19 m, a wall thickness of 15 mm, and a length of 2.29 m that is modeled with shell elements. The same plastic kinematic material model developed for the mild reinforcement in the bridge was assigned to the steel tank. The concrete pipe model is an open ended hollow cylinder with a wall thickness of 178 mm and the same outside diameter and length as the steel tank. Solid elements were used to model the concrete pipe with the CSCM constitutive model. Erosion settings for the concrete of the impactor and the girders were established such that erosion occurs when the damage exceeds 0.99 and the maximum principal strain exceeds 0.1. The automatic surface-to-surface contact card was used to model contact between the respective impactor and girder.

A set of simulations were performed with each impactor model to preliminarily investigate the variation in the impact force characteristics and damage to the girder with the impact location and impactor velocity. For each impactor, nonlinear transient analysis was conducted for impacts occurring at the quarter point, third point, and midspan of the bridge. The midspan location is coincident with the location of the intermediate diaphragm. For each impact location, simulations were performed for impactor velocities of 72.4 km/h, 88.5 km/h, 104.6 km/h, and 120.7 km/h. All simulations were performed for a termination time of 300 ms to ensure that all significant dynamics were completed by the end of the analysis. Time histories for the lateral displacements at the respective impact location were used to confirm this. For all cases investigated, the top of the tank or pipe was located 330 mm above the base of the bottom flange of the girder. The total mass of the steel tank model is 2795 kg and the estimated contact area associated with the impact to the bottom flange of the girder is 2622 cm^2. The total mass of the concrete pipe model is 6171 kg and the estimated contact area associated with the impact to the bottom flange of the girder is 1690 cm^2. The output time interval for the contact force time histories was $1x10^{-5}$ s.

The typical variation in impact force time history across the impactor velocities is presented in Figure 3. The duration of the time histories plotted in this figure is truncated to 6 ms, as this is the time window over which the magnitudes of the impact forces are significant. The FE results presented in this figure were obtained with the steel tank model, but similar observations were made with the simulation data obtained with the concrete pipe model. As expected, the peak force and impulse increases as the velocity of the impactor increases. Figure 4 presents impact force time histories for collisions of the concrete pipe with a velocity of 104.6 km/h at the three different locations in the span. The results suggest that neither the peak force nor the impulse are sensitive to the location of the impact in the bridge span. Similar results were obtained for the other velocities as well as for the simulations performed with the steel tank model. The duration of the impact is also approximately twice as long as that presented in Oppong et al. (2021a). The longer contact duration may be the result of a more flexible girder, which is the result of the significantly longer span length of the bridge modeled in the current paper as well as the complete modeling of the superstructure.

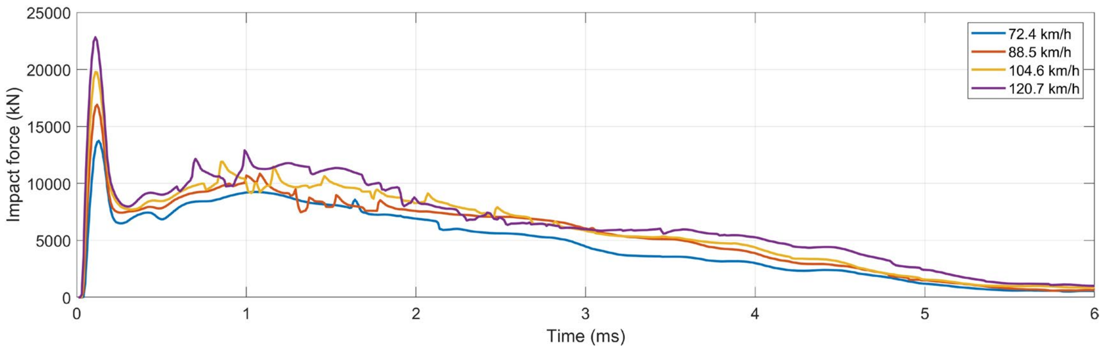

Figure 3. Impact force time histories for steel tank collision at midspan of the bridge.

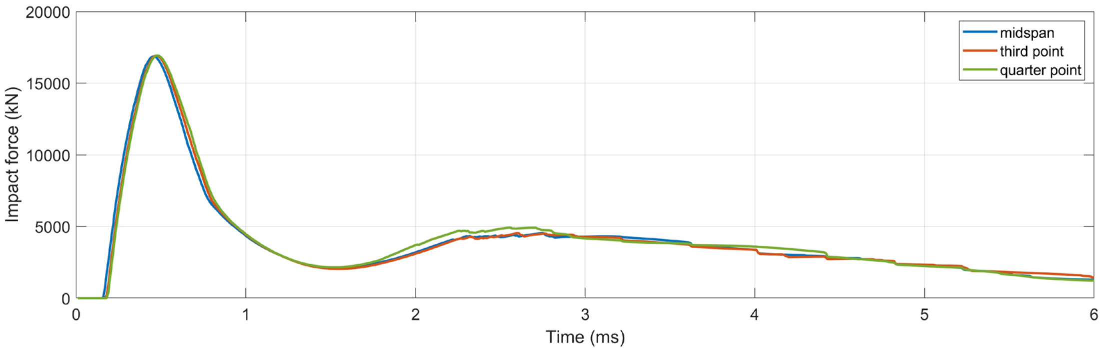

Figure 4. Impact force time histories for concrete pipe collisions with velocity of 104.6 km/h.

As previously mentioned, Oppong et al. 2021a developed a set of prediction equations for the peak and mean impact forces developed by collisions of steel tanks and concrete pipes based on parametric analysis conducted with a reinforced concrete girder model. In this referenced paper, the mean impact force was defined as the impulse divided by the duration of the impact. In the current study, the peak impact forces were extracted from the force time histories and the mean impact forces were calculated by numerical integration. Figure 5 presents a comparison between the results from the 24 FE simulations and the predictions developed with the simplified equations. These preliminary results suggest that the prediction equation significantly overpredicts the peak forces from the steel tank when extended to this case study. However, the peak impact forces developed for the concrete pipe exhibit reasonably strong agreement with the prediction equation. Conversely, the mean impact forces, or impulse, developed by the FE simulations with the steel tank agree well with the prediction equation, while the mean impact forces from the simulations with the concrete pipe are significantly lower than the anticipated by the prediction equation.

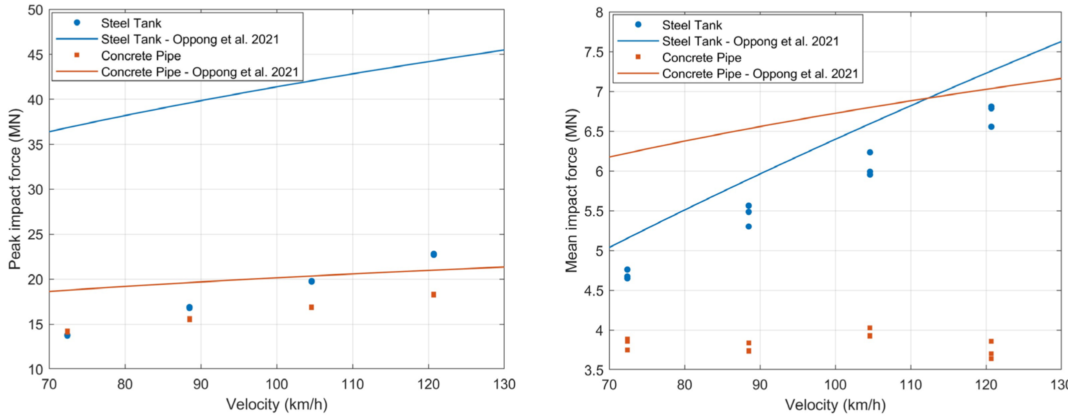

Figure 5. Comparison between FE results from high-fidelity bridge model and prediction equations: a) peak impact force; b) mean impact force.

Figure 6 presents the condition of the exterior girder at the end of the simulation for the four different velocities of the steel tank collision at the quarter point and the midspan. The fringe pattern depicted in the figure and indicated in the legend is the maximum principal strain. Some erosion of elements can be observed for the greater levels of damage severity. The simulations predict damage in the form of spalling and loss of side cover at the contact area, lateral and torsional deformation of the impacted girder, localized loss of prestress and a significant crack extending up to the top of the web of the girder. In general, the damage patterns are consistent with expectations based on documented field observations (Feldman et al. 1996). While some differences are apparent in the damage produced at different impact locations, the FE results suggest that the velocity of the impactor has a more significant influence on the severity of damage than the impact location. In this limited preliminary study, the authors found that the presence of the steel intermediate diaphragm reduced the extent of lateral displacement for impacts at the midspan. Lastly, it is noted that the degree of damage apparent in the FE simulations is significant, however Oppong et al. (2021a) pointed out that the steel tank and concrete pipe impactor models generated significantly greater impact forces and greater damage than their other models of construction objects or the tractor semi-trailer model. Future extension of this work will expand the simulation database to include additional impactors as well as additional bridge models.

4 CONCLUSION

This paper presented a high-fidelity approach to modeling prestressed concrete girder bridges and simulating the collision of vehicles and construction objects. Preliminary results obtained from a set of 24 simulations performed with two different impactors, three different impact locations, and four different speeds suggest that the characteristics of the impact force time history are not affected by the location of the impact. Comparison of the impact force time histories with a set of prediction equations from the literature developed with a reinforced concrete beam model yielded mixed results. Based on this limited preliminary investigation, the severity of damage to the girder appears to be affected more significantly by the velocity of the impactor than the location of the impact. Early evidence from the study indicates that steel intermediate diaphragms result in reduced lateral deformation for impacts occurring near the diaphragm.

Figure 6. Damage pattern across exterior girder for steel tank with velocity of 72.4 km/h, 88.5 km/h, 104.6 km/h, and 120.7 km/h: (a) impact at quarter point of span; (b) impact at midspan.

REFERENCES

Abendroth, R., Klaiber, F., & Shafer, M. 1995. Diaphragm effectiveness in prestressed-concrete girder bridges. *Journal of Structural Engineering* 121(9): 1362-1369.

Adhikary, S., Li, B., & Fujikake, K. 2015. Low Velocity Impact Response of Reinforced Concrete Beams: Experimental and Numerical Investigation. *International Journal of Protective Structures*, 6 (1): 81–111. SAGE Publications. https://doi.org/10.1260/2041-4196.6.1.81.

Agrawal, A., Xu, X. & Chen, Z. 2011. *Bridge-vehicle impact assessment*. Final report number C-07-10, University Transportation Research Center, New York State Department of Transportation (UTRC/NYSDOT).

Cai, C., Araujo, M., Chandolu, A., Avent, R., & Alaywan, W. 2007. Diaphragm effects of prestressed concrete girder bridges: review and discussion. *Practice Periodical on Structural Design and Construction* 12(3): 161-167.

Cook, W., Barr, P., & Halling, M. 2015. Bridge failure rate. *Journal of Performance of Constructed Facilities* 29(3): 04014080-1.

Feldman, L., Jirsa, J., Fowler, D., & Carrasquillo, R. 1996. *Current Practice in the Repair of Prestressed Bridge Girders*. Center for Transportation Research, The University of Texas at Austin, FHWA/TX-96/1370-1.

Jiang, H. & Chorzepa. 2015. An effective numerical simulation methodology to predict the impact response of pre-stressed concrete members. *Engineering Failure Analysis* 55: 63-78.

Jing, Y., Ma, Z., & Clarke, D. 2016. Full-scale lateral impact testing of prestressed concrete girder. *Structural Concrete*. 17(6): 947-958.

National Center for Statistics and Analysis. 2022. *Traffic Safety Facts 2020: A Compilation of Motor Vehicle Crash Data*. 242. National Highway Traffic Safety Administration.

Oppong, K., Saini, D. & Shafei, B. 2021a. Characterization of impact-induced forces and damage to bridge superstructures due to over-height collision. *Engineering Structures* 236: 112014

Oppong, K., Saini, D. & Shafei, B. 2021b. Ultrahigh-performance concrete for improving impact resistance of bridge superstructures to overheight collision. *Journal of Bridge Engineering* 26(9): 04021060

Qiao, P., Yang, M., & McLean, D. 2008. *Effect of Intermediate Diaphragms to Prestressed Concrete Bridge Girders in Over-Height Truck Impacts*. Washington State Transportation Center (TRAC).

Saini, D. & Shafei, B. 2019. Concrete constitutive models for low velocity impact simulations. *International Journal of Impact Engineering* 132: 103329.

Whelan, M. & Janoyan, K. 2012. Assessment of simplified linear dynamic analysis of a multispan skew bridge on steel-reinforced elastomeric bearings. *Journal of Bridge Engineering* 17(1): 151-160.

Xu, L., Lu, X., Guan, H., & Zhang, Y. 2013. Finite-element and simplified models for collision simulation between overheight trucks and bridge superstructures. *Journal of Bridge Engineering* 18(11): 1140-1151.